Hindawi
Advances in Civil Engineering
Volume 2022, Article ID 9291890, 15 pages
https://doi.org/10.1155/2022/9291890

Research Article

Effect of Mean Grain Size on the Small-Strain Dynamic Properties of Calcareous Sand

Liwei Wen [1,2,3]

[1]*Key Laboratory of Earthquake Engineering and Engineering Vibration, Institute of Engineering Mechanics, China Earthquake Administration, Harbin, Heilongjiang 150080, China*
[2]*Key Laboratory of Earthquake Disaster Mitigation, Ministry of Emergency Management, Harbin, Heilongjiang 150080, China*
[3]*School of Civil Engineering, Guangzhou University, Guangzhou, Guangdong 510006, China*

Correspondence should be addressed to Liwei Wen; liweiwen@gzhu.edu.cn

Received 7 May 2022; Accepted 29 June 2022; Published 18 July 2022

Academic Editor: Chao Zou

Calcareous sand was selected as the prior material for island reclamation in many coastal regions. The mechanical properties of the granular materials are greatly affected by their grain size distribution conditions. The shear modulus and damping ratio are two important parameters for earthquake ground response analysis and liquefaction evaluation. A series of resonant column tests had been performed on calcareous sands with varying median grain diameter and uniform coefficient. The dependence of the shear modulus and damping ratio of the calcareous sand on grain size has been confirmed in this examination. The test results reveal that the shear modulus decreases with a rise in shear strain for calcareous sand samples at a given confining pressure and relative density. The maximum shear modulus tends to increase with confining pressure and relative density. On the maximum shear modulus and void ratio plane, the trend lines of the measured results shift toward up and right position with a rise in grain diameter. The measured results indicate that the influence of uniform coefficient on the maximum shear modulus is neglectable. A revised empirical equation based on the Hardin model had been proposed considering the influence of grain diameter to estimate the maximum shear modulus of calcareous sand. The predicted values show satisfactory agreement with the measured results. The results manifest that the effect of grading condition on small-strain dynamic properties of calcareous sands cannot be neglected for the evaluation of seismic safety for reclamation engineering sites.

1. Introduction

Calcareous sands are biogenic medium and widely distributed in the coastal region all around the world. They are originated from marine shells and organisms. The major composition of such marine medium is calcium carbonate. The calcareous sands possess an intrapore structure, angular shape, and a rough surface. The calcareous sands are liable to be damaged at normal working stress [1–4]. Thus, calcareous sediments exhibit different mechanical response compared to the terrigenous sand. Recently, the calcareous sand is selected as the prior material for reclamation construction. The demand for fundamental understanding of the mechanical properties of calcareous sand is highly urgent.

Some costal island reclamation work in South China Sea had been constructed in past years [5–8]. Besides, the occurrence of earthquakes is frequently reported in that area. Therefore, well understanding of the dynamic characteristic of the sand deposition site is significantly important for the earthquake of reef reclamation site. Moreover, the small-level dynamic properties are parameters affecting the ground motion characteristics. Those indexes can also be adopted to estimate the settlement of reclamation ground subjected to earthquake.

The shear stiffness of the sand at the shear strain level less than 10–5 is generally defined as Go. Past studies verified that the shear modulus was the function of void ratio and confining stress. Additionally, the small-level dynamic properties of sand are also susceptible to many other factors including gradation, distribution, and particle characteristics. The bender element and resonant column tests are the two tradition laboratory approaches to measure the small-

level dynamic index of sands. The resonant column tests had been extensively carried out to measure the small-level dynamic properties of sands [9–12]. Phamet al. [13] found that the maximum shear modulus of the calcareous was larger than that of silica sand under the same test condition. Goudarzy et al. [14] noticed that the maximum shear modulus significantly reduced with increasing fines content and adopted the equivalent skeleton void ratio [15] to revise the Hardin model [16] to include the effect of fines particles on fabric and force chains of sand assembly. Jafarian and Javdanian [17] tested the dynamic properties of siliceous-carbonate sand and understood that the maximum shear modulus of the samples subjected to anisotropic condition was larger than the isotropically consolidated samples. The effect of uniform coefficient and mean grain size on the dynamic properties of sand at the small-strain level is mixed. Anastasiadis et al. [18] reported that the mean grain size affected the normalized shear modulus of the sand. However, some researchers held the opposite opinions [19, 20]. Therefore, the investigation on the effect of grain diameter on the small-level dynamic properties of the calcareous sand is still insufficient. Further research should be conducted to complement the existing literature.

This study carries out a series of resonant column tests to examine the influences of median diameter and uniform coefficient on the shear modulus and damping ratio of the calcareous sand at different confining pressures and densities. The dependence of the shear modulus of calcareous sand on the void ratio and confining pressure plane is also studied. The test results indicate that the effect of gradation condition on the small-strain dynamic properties of calcareous sand should be seriously considered when the earthquake ground response analysis and liquefaction evaluation of reclamation site are conducted. The well-proved Hardin model [16, 21] had been revised to consider the effect of gradation condition to estimate the maximum shear modulus of calcareous sand under different test conditions. The predicted values agree well with measured results for calcareous sand with varying gradation conditions.

2. Materials and Methods

The calcareous sand was collected from the Nansha island, South China Sea. The grain size distribution range for the calcareous sand of the Nansha island region is quite wide, and these biogenetic sediments contain large and small grains by arbitrary proportion. To investigate the influence of gradation property on the small-strain dynamic characteristics of calcareous sand, the grain size distribution curves of calcareous sand had been artificially adjusted. Figure 1 shows the grain size distribution curves of all samples. Three median diameters (d_{50}) of 0.75 mm, 1.5 mm, and 2.5 mm had been selected. For each grain diameter, the uniform coefficient Cu had been prepared as 1.2, 1.8, and 2.4. The larger the uniform coefficient Cu is, the wider the grain size distribution curve becomes. The grading curve basically covers the representative grain size distribution range in the reclamation reef island. It is noticed that less fines particle with a grain diameter smaller than 0.075 mm exist in tested

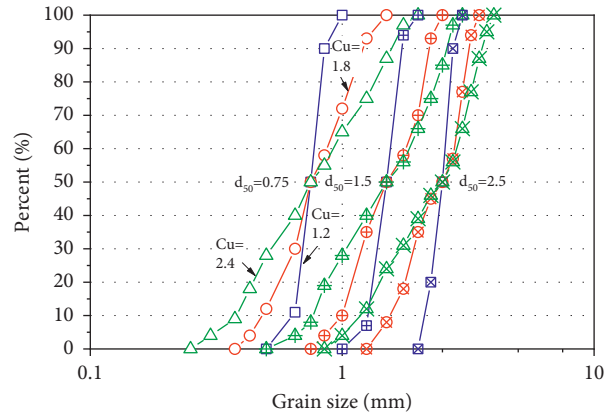

Figure 1: Grain size distribution curves of calcareous sand with varying gradation conditions.

Table 1: The physical parameters of calcareous sand with different gradation conditions.

Sample no.	e_{max}	e_{min}	d_{50} (mm)	C_u	G_s
1	1.264	0.902	0.75	1.2	2.76
2	1.279	0.854	0.75	1.8	2.76
3	1.214	0.774	0.75	2.4	2.76
4	1.273	0.968	1.5	1.2	2.76
5	1.139	0.896	1.5	1.8	2.76
6	1.072	0.835	1.5	2.4	2.76
7	1.390	1.084	2.5	1.2	2.76
8	1.295	1.006	2.5	1.8	2.76
9	1.233	0.970	2.5	2.4	2.76

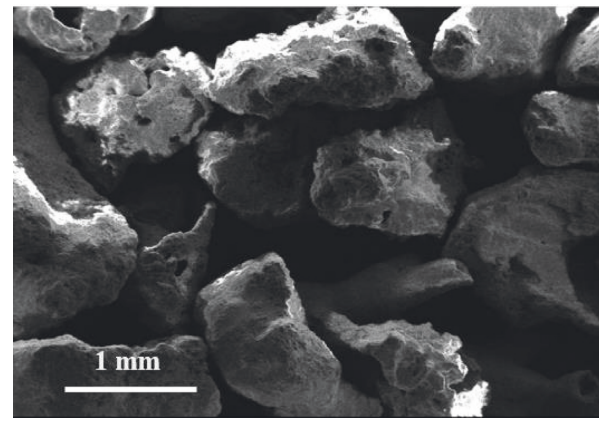

Figure 2: Scanning electron microscopy of calcareous sand.

materials [22–24]. Table 1 shows the representative physical parameters of the calcareous sand with varying median diameters and uniform coefficients. It is noted that the maximum and minimum void ratios of calcareous sand are affected by the gradation condition. For the same median diameter d_{50}, both the maximum and minimum void ratios decrease as coefficient uniform Cu increases. The maximum and minimum void ratios also increase as the median diameter increases. It is because more void space is created for the skeleton structure formed by large grains. The specific

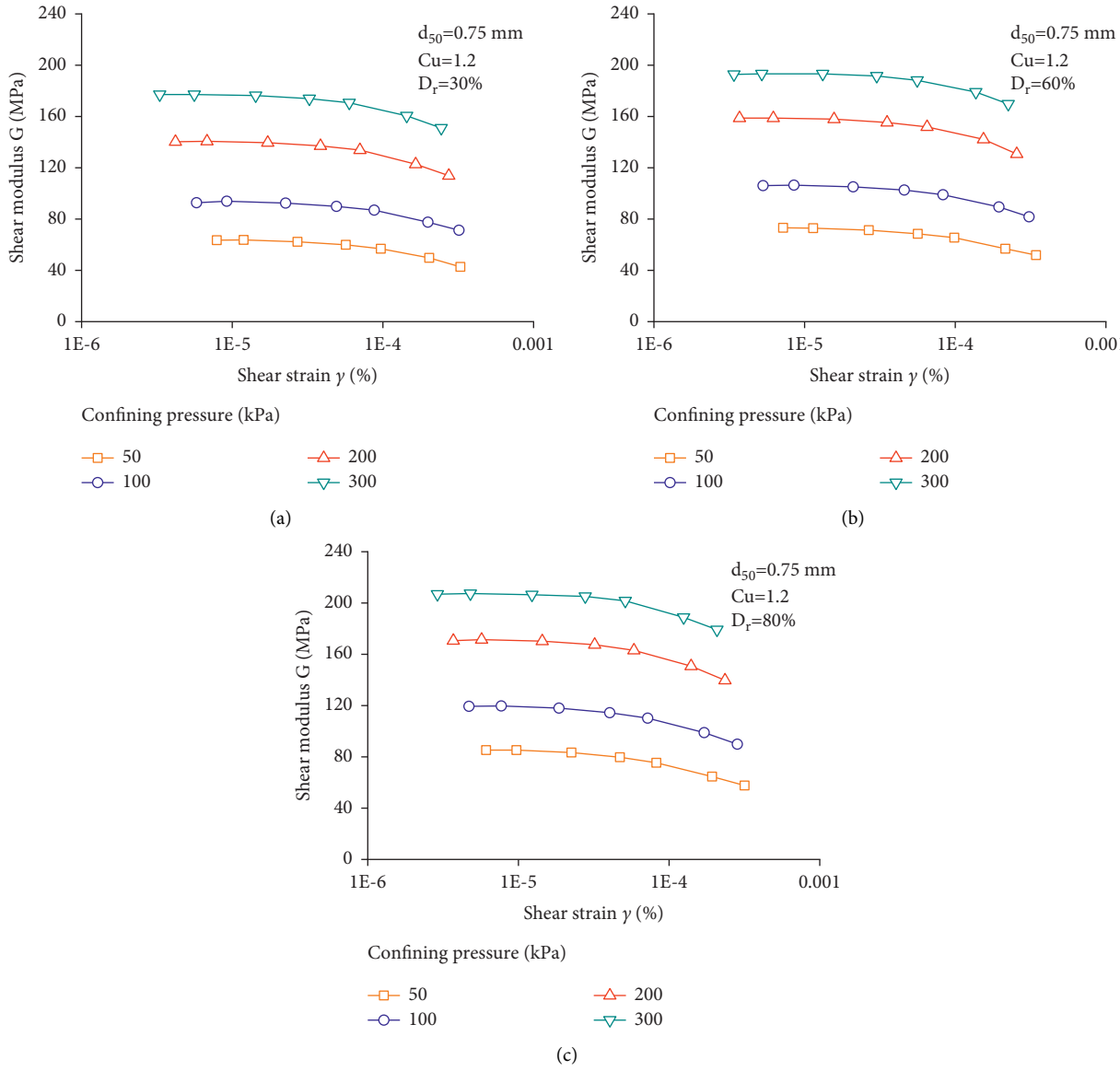

FIGURE 3: Shear modulus G and shear strain γ for calcareous sand with $d_{50} = 0.75$ mm and Cu = 1.2 at different confining pressures. (a) Loose state. (b) Medium dense state. (c) Dense state.

gravity G_s is less dependent on the median diameter and uniform coefficient.

Figure 2 shows the scanning electron microscopy of calcareous sand grains. The image shows that the particle shape of the calcareous sand is irregular and complex. The pores are distributed on the grain surface, and some pores are connected into the internal portion. The grain surfaces seem quite rough. The complex grain shape and microstructure of calcareous sand make its dynamic properties quite different from terrigenous sands.

The calcareous sand samples were prepared using the wetting tamping method [25–31]. The calcareous sand was mixed with an initial water content of 10%. The cylindrical sample is 50 mm in diameter and 100 mm in height. The moist calcareous sand was gradually poured into mold by five layers. The samples were prepared at different densities by specific tamping times. Three target relative densities of samples as 30% (loose state), 60% (medium-dense state), and 80% (dense state) were prepared. The saturation process for the calcareous sand sample is difficult due to its porositic nature. Initially, the calcareous sand is kept in vacuum for de-air. CO_2 is injected into the calcareous sand sample to replace the air, and this process lasts for 45 minutes. The saturation process for calcareous sand sample is accomplished by gradually elevating the back pressure. The Skempton B value for all samples is over 0.95 before testing. The isotropic consolidation pressures are set as 50 kPa, 100 kPa, 200 kPa, and 300 kPa before testing.

The GDS resonant column testing apparatus had been adopted to study the small-strain dynamic response of calcareous sand in this investigation. The resonant column testing apparatus is classified into the Stokoe type. The sample is excited in sinusoidal vibrations. The confining and back pressure range are 1.0 MPa, and the operating frequency

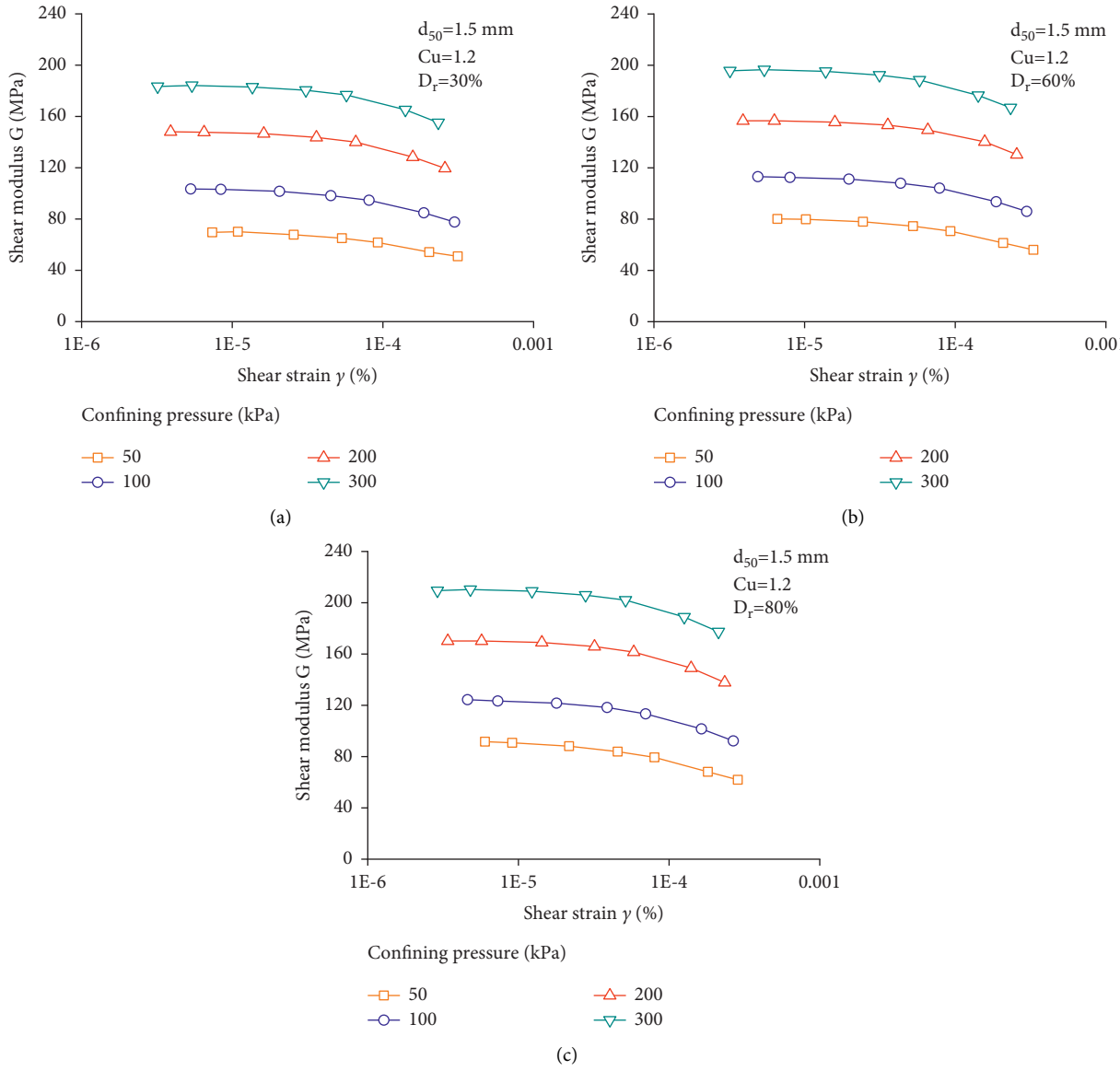

FIGURE 4: Shear modulus G and shear strain γ for calcareous sand with $d_{50} = 1.5$ mm and Cu = 1.2 at different confining pressures. (a) Loose state. (b) Medium dense state. (c) Dense state.

range is between 5 and 30 Hz. The cylindrical sample is installed in triaxial cell, and the cell base is embraced by water in an inner tube.

3. Test Results

Figure 3 shows the shear modulus G-shear strain γ curve of calcareous sand with a median diameter of 0.75 mm and a uniform coefficient Cu = 1.2 at three densities of 30%, 60%, and 80%. The varying range of shear modulus measured in this study is between $5 * 10^{-5}$ and 10^{-4}. The test results display that the shear modulus G tends to decline with a rise in the shear strain regardless of the initial relative density. The attenuating tendency of the shear modulus is steady at a small-level shear strain and intensifies as the shear strain increases. The confining stress-dependence of the shear modulus for calcareous sand is also clearly seen. At a specific confining pressure, the shear modulus-shear strain curves move upward with a rise in relative density. The varying range for the shear modulus of calcareous sand at loose, medium-dense, and dense states is between 40 MPa and 210 MPa.

Figures 4 and 5 present the plot of shear modulus G against the shear strain γ of calcareous sand with median diameters of 1.5 mm and 2.5 mm at varying confining pressures and densities. The shear modulus-shear strain curves expressed in Figures 4 and 5 exhibit quite similar varying tendency to the calcareous sand with a small median grain diameter shown in Figure 3. A rise in the confining pressure largely elevates the position of the G-γ curve. A rise in deposition state markedly enhances the shear modulus under the same test condition. It demonstrates that the densification of the calcareous sediment is an effective approach to increase the resilience of the reclamation ground when the earthquake occurs.

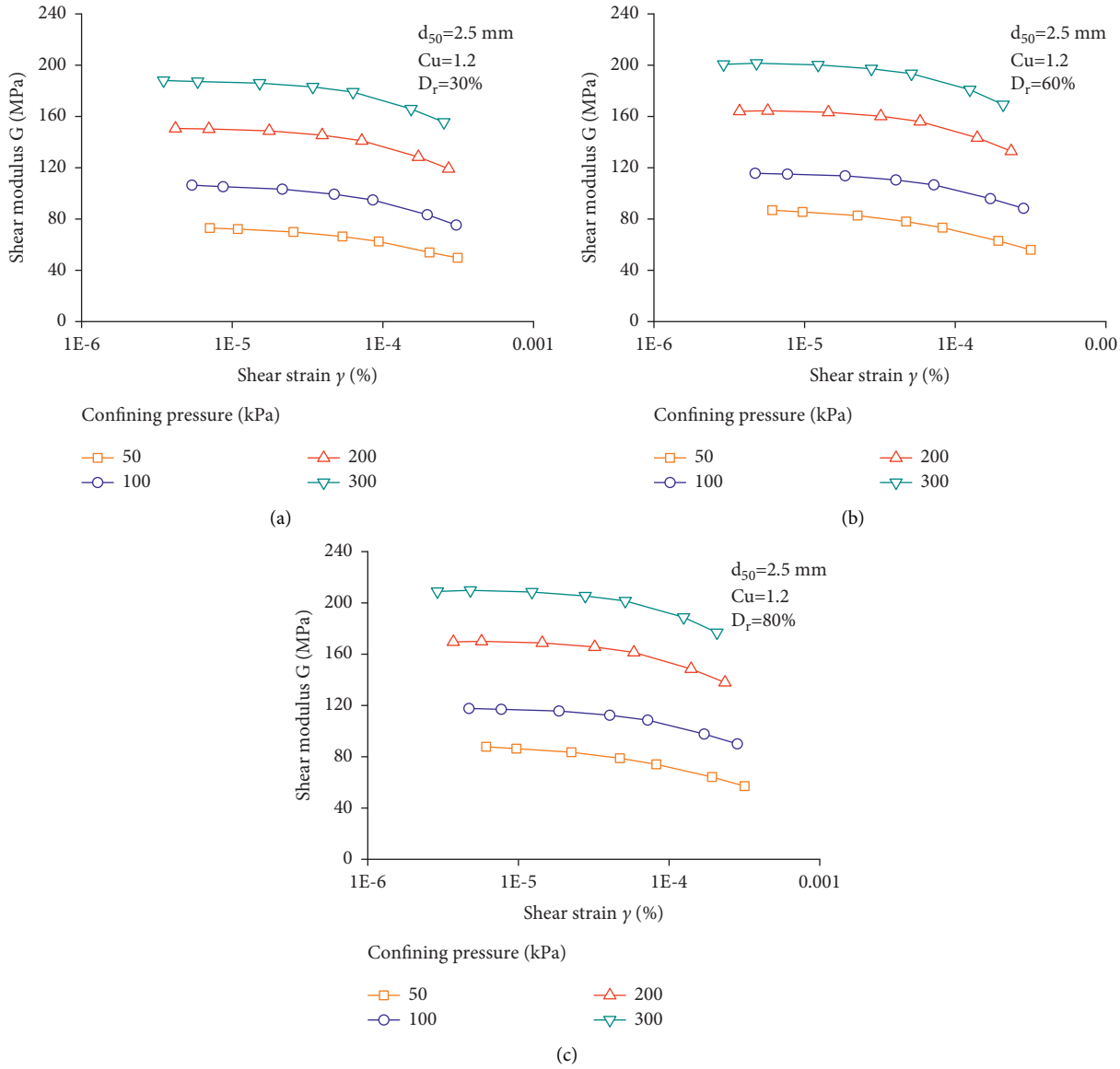

FIGURE 5: Shear modulus G and shear strain γ for calcareous sand with $d_{50} = 2.5$ mm and Cu = 1.2 at different confining pressures. (a) Loose state. (b) Medium dense state. (c) Dense state.

Figures 6(a) and 6(b) show the varying tendency of maximum shear modulus G_o with the level of confining stress for calcareous sand samples with median diameters of 0.75 mm and 2.5 mm, respectively. The maximum shear modulus G_o is determined as the intersection point of vertical axis and the fitting curve to measured data on shear modulus and shear strain γ plane. The dependence of maximum shear modulus G_o on the stress and density levels is distinctive. It is seen that the maximum shear modulus G_o linearly increases with a rise in confine pressure. An increasing confining pressure makes the calcareous sand grains closely contacted during the isotropic consolidation process. A rise in relative density enhances the maximum shear modulus for calcareous sand sample with small and large grains. Confining stress and deposition state are two influential parameters determining the maximum shear modulus for sandy material. It indicates that a denser calcareous ground owns a stronger modulus to resist small-level vibration loading. The results are consistent with past investigations on silica and calcareous sands [9, 32].

Figures 7(a) and 7(b) show the maximum shear modulus G_o plotted against the median diameter d_{50} for the calcareous sand. For calcareous sand with a uniform coefficient Cu = 1.2, the maximum shear modulus G_o is insensitive to the grain size at both loose and dense states. However, for calcareous sand with a relatively larger uniform coefficient, the maximum shear modulus G_o initially increases and reverses to reduce with diameter varying from 0.8 to 2.4. For a well-graded calcareous sand with a specific median diameter, the total grain number within a specimen and the major "force chain" subjected to torsion are larger than the other two cases. It is supposed that the mechanism about the influences of grain size and gradation condition on the small-level dynamic shear modulus is quite complicated.

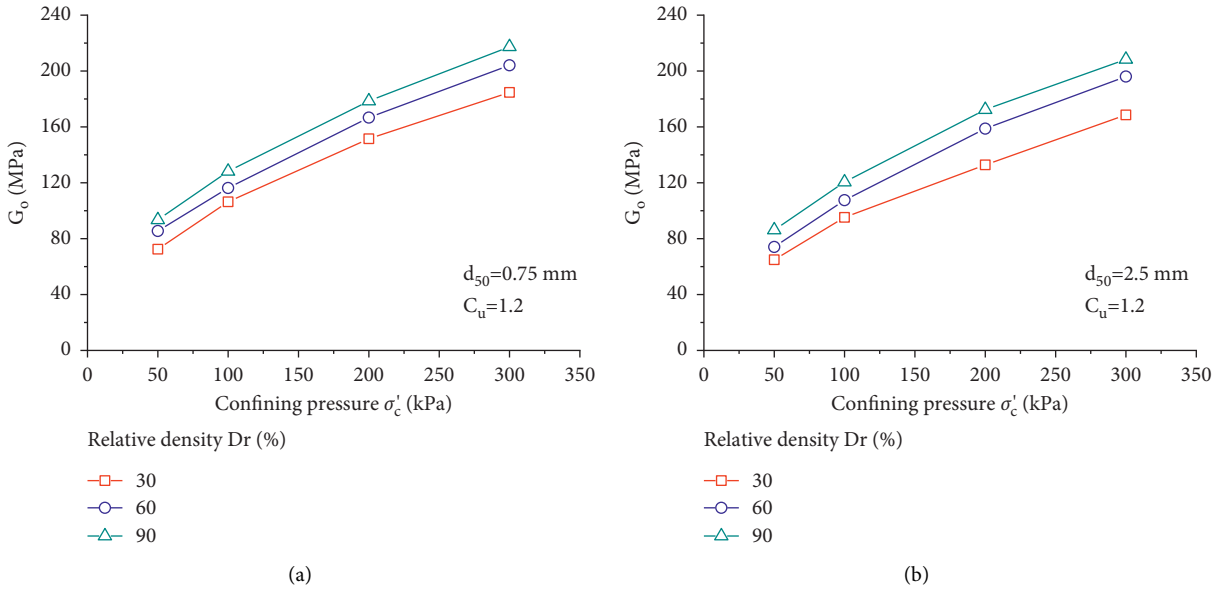

Figure 6: Maximum shear modulus G_o and confining pressure for calcareous sands with Cu = 1.2 at varying densities. (a) d_{50} = 0.75 mm and (b) d_{50} = 2.5 mm.

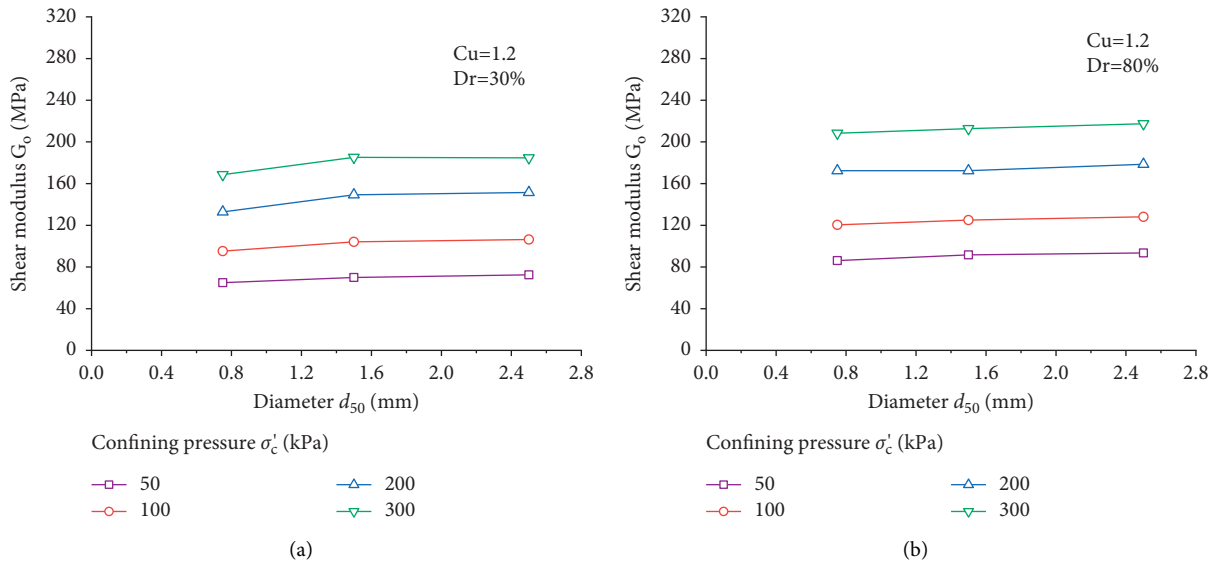

Figure 7: Continued.

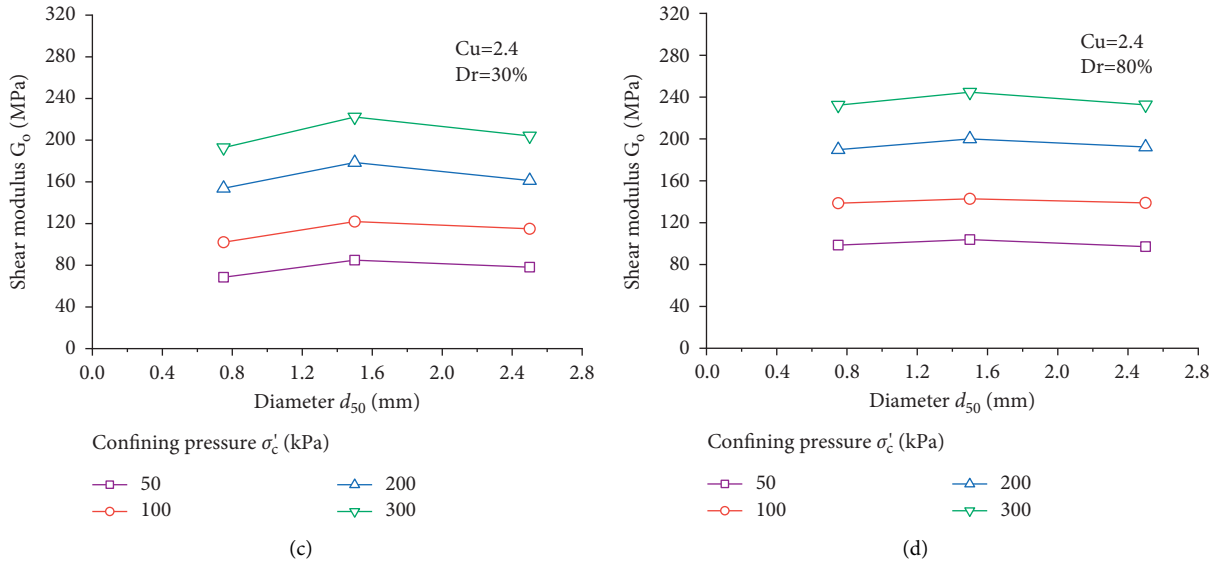

Figure 7: Maximum shear modulus G_o and median diameter d_{50}. (a) Cu = 1.2, Dr = 30%; (b) Cu = 1.2, Dr = 80%; (c) Cu = 2.4, Dr = 30%; (d) Cu = 2.4. Dr = 80%.

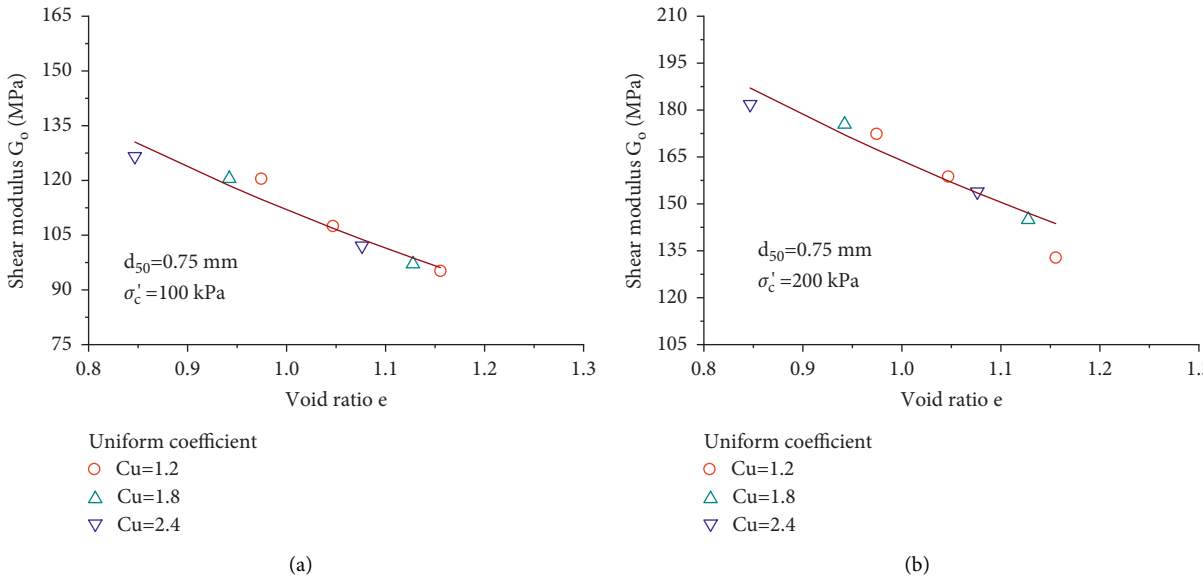

Figure 8: Continued.

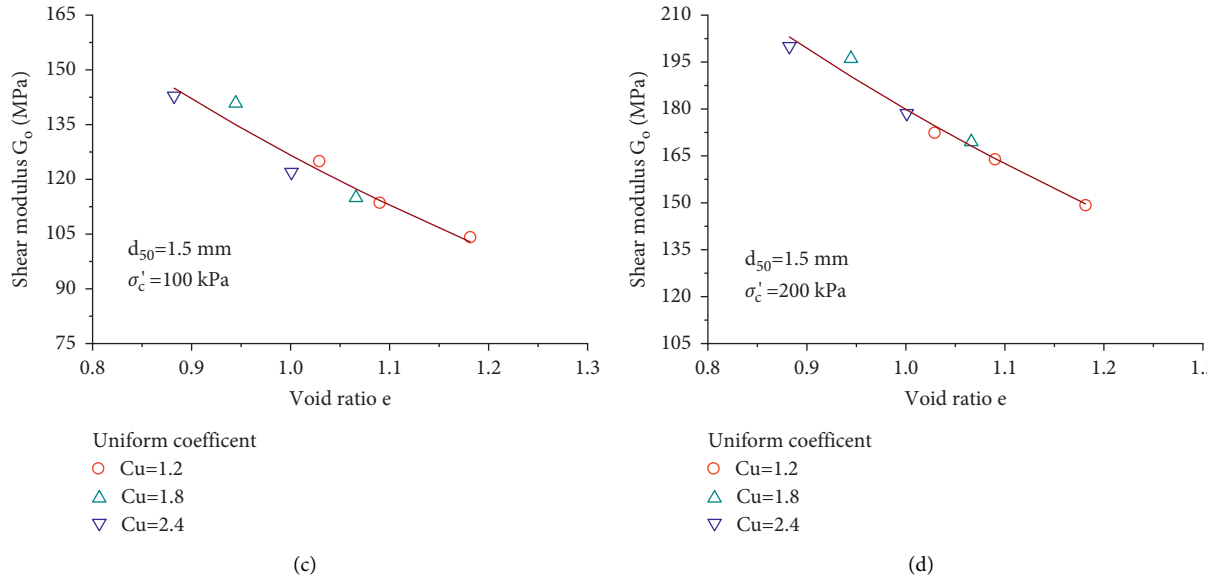

Figure 8: Shear modulus and void ratio for calcareous sand with varying uniform coefficient Cu. (a) $d_{50} = 0.75$ mm, 100 kPa; (b) $d_{50} = 0.75$ mm, 200 kPa; (c) $d_{50} = 1.5$ mm, 100 kPa; (d) $d_{50} = 1.5$ mm, 200 kPa.

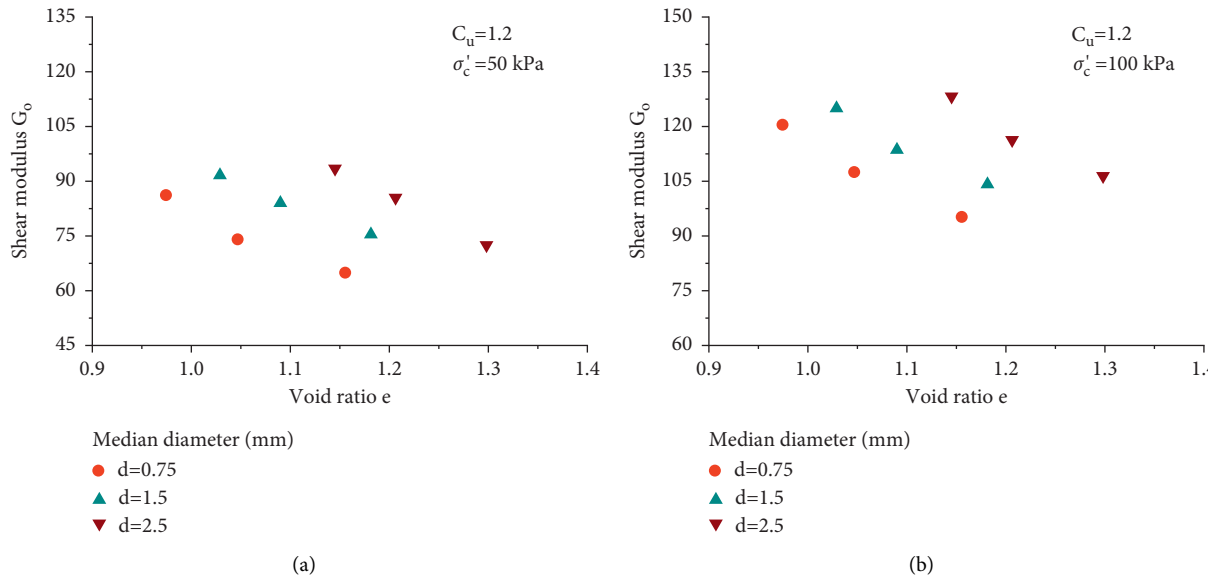

Figure 9: Continued.

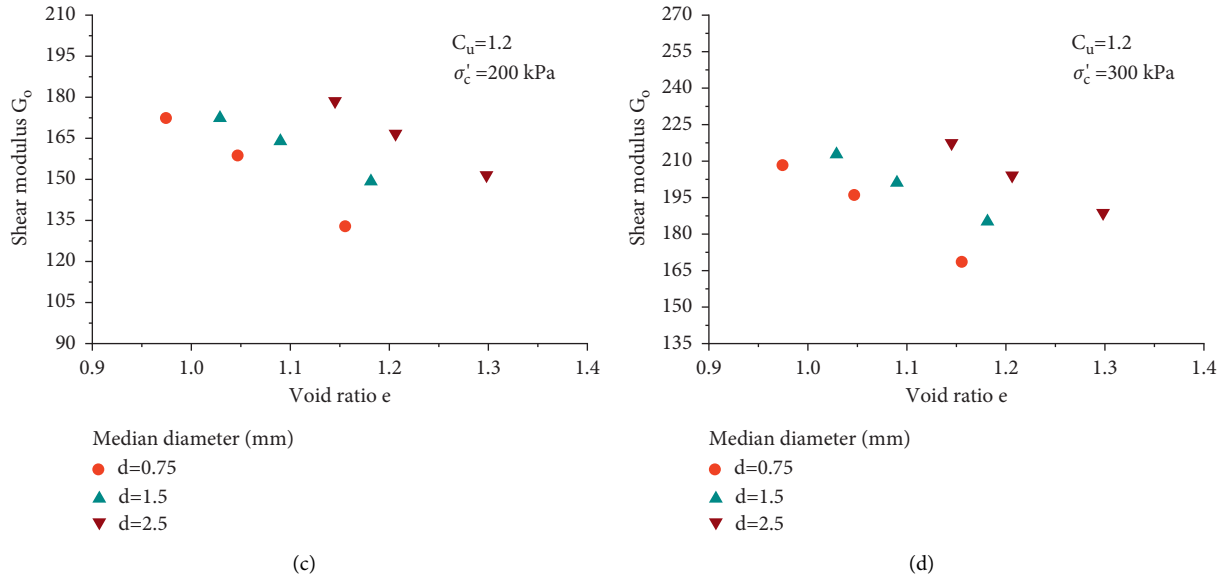

Figure 9: Maximum shear modulus and void ratio for calcareous sand with Cu = 1.2. (a) 50 kPa, (b) 100 kPa, (c) 200 kPa, and (d) 300 kPa.

Further investigation should be carried out to reveal the relevant micromechanism.

To directly understand the effect of uniform coefficient Cu on the maximum shear modulus, the test data under different test conditions are compared on the maximum shear modulus G_o-void ratio e plane. Figure 8 shows the relationship between the maximum shear modulus and void ratio for calcareous sand with varying uniform coefficient. The maximum shear modulus G_o tends to decrease with a rise in the void ratio. The calcareous sands subjected to dynamic loading loses its deformation resistance ability when it is at a loose state. It is noted that the effect of uniform coefficient on the G_o-e curve is neglectable. In Figure 8, all test results could be simulated using a curve on the maximum shear modulus and the void ratio plane when the median diameter and confining pressure are known. The test results acquired in this work are different to previous investigations on silica sand [11, 33]. The difference is probably originated from the grain morphology between the calcareous sand and silica sand.

Figure 9 expresses the maximum shear modulus G_o plotted against the void ratio e for calcareous sand with uniform coefficient Cu = 1.2 and different median diameters. The vertical axis for Figures 9(a)–9(d) is different because the applied confining pressure level is different. With similarity to Figure 8, the maximum shear modulus displays reducing tendency as the sample becomes loose. Under the same test condition, the effect of the grain diameter on the maximum shear modulus G_o is remarkable on the G_o-e plane. It is clearly seen that a decrease in grain diameter d makes the measured result points move downward. The difference in the grain diameter leads to the different fabric and coordination number among the grain particles. The complex contact condition in samples with small grain diameter leads to the reduction in maximum shear modulus for calcareous sand [34–38].

Figures 10 and 11 show the relationship between the maximum shear modulus G_o and void ratio e for calcareous sands at different confining pressures and two uniform coefficients. It indicates that the maximum shear modulus reduces as samples become loose. Besides, a rise in the grain diameter increases the maximum shear modulus at the same void ratio although only two measured points are acquired for a given median diameter. It is noted that the dependence of maximum shear modulus G_o on the grain size is applicable for samples with different Cu. Therefore, the effect of median diameter on the dynamic index of calcareous sand should be reasonably treated when the estimation equation of the maximum shear modulus is proposed.

4. Discussion

Past studies revealed that the shear modulus of the sand was greatly dependent on the density and confining stress [39–43]. Hardin and Richart [21] proposed an empirical formula to estimate the shear modulus G_o of sandy soil based on a database. The shear modulus G_o could be expressed as follows:

$$\mathrm{Go} = A\frac{(\mathrm{c}-\mathrm{e})^2}{1+e}\left(\frac{p}{p_a}\right)^n, \quad (1)$$

where A, n, and c are the material constant. p_a represents atmospheric pressure (100 kPa), and p indicates the consolidation stress. Additionally, parameter c is affected by the angularity of the grains and takes the value of 2.97 for angular sand. The item related with void ratio e is also expressed by other forms in some studies.

Figure 12 shows the $G_o/(p/p_a)^{0.5} - e$ curve of calcareous sand using three median diameters. The normalization form of vertical axis is adopted to eliminate the effect of confining stress. The points representing the test results with the same Cu at different confining pressures are closely distributed.

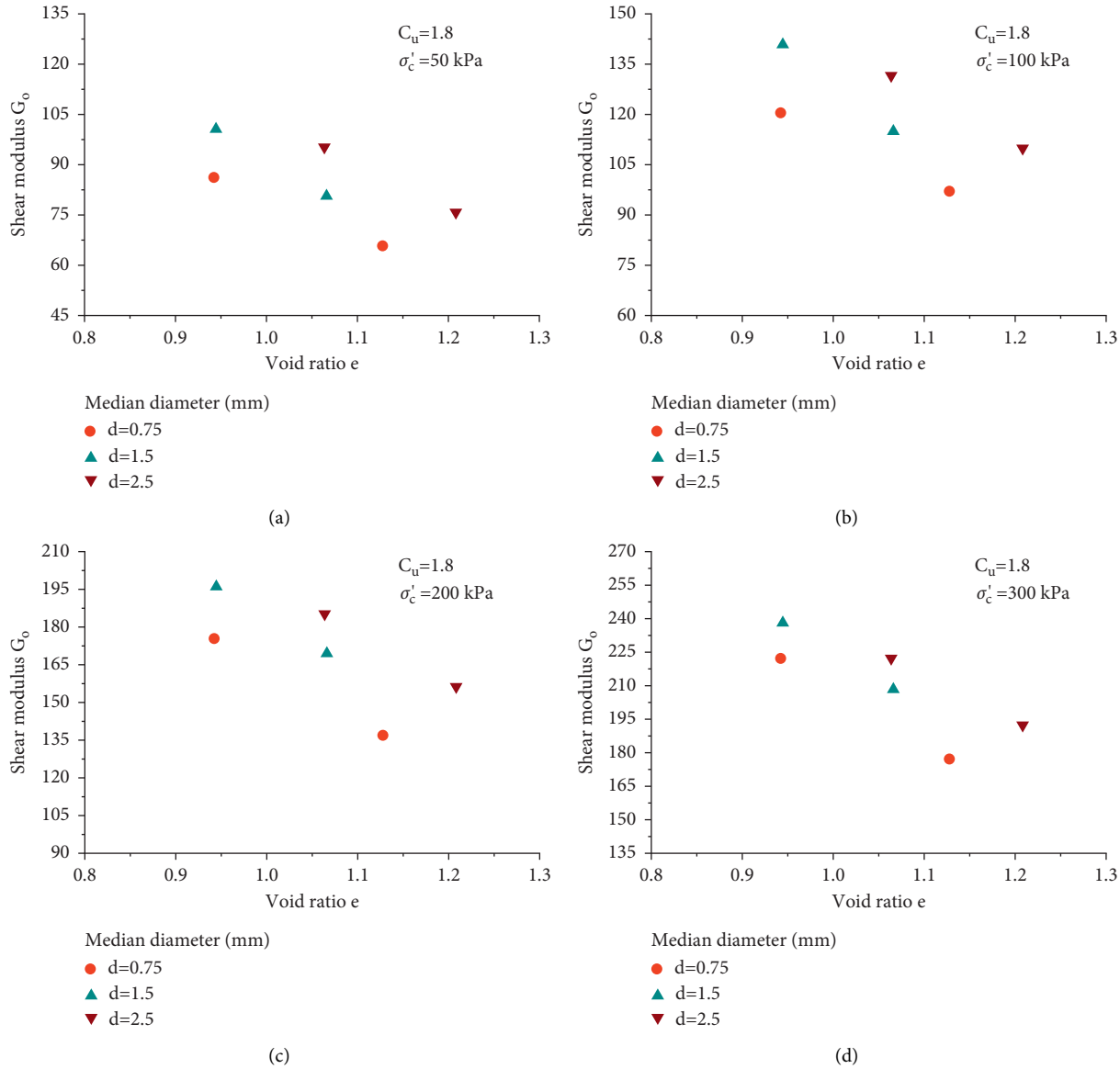

Figure 10: Maximum shear modulus and void ratio for calcareous sand with Cu = 1.8. (a) 50 kPa, (b) 100 kPa, (c) 200 kPa, and (d) 300 kPa.

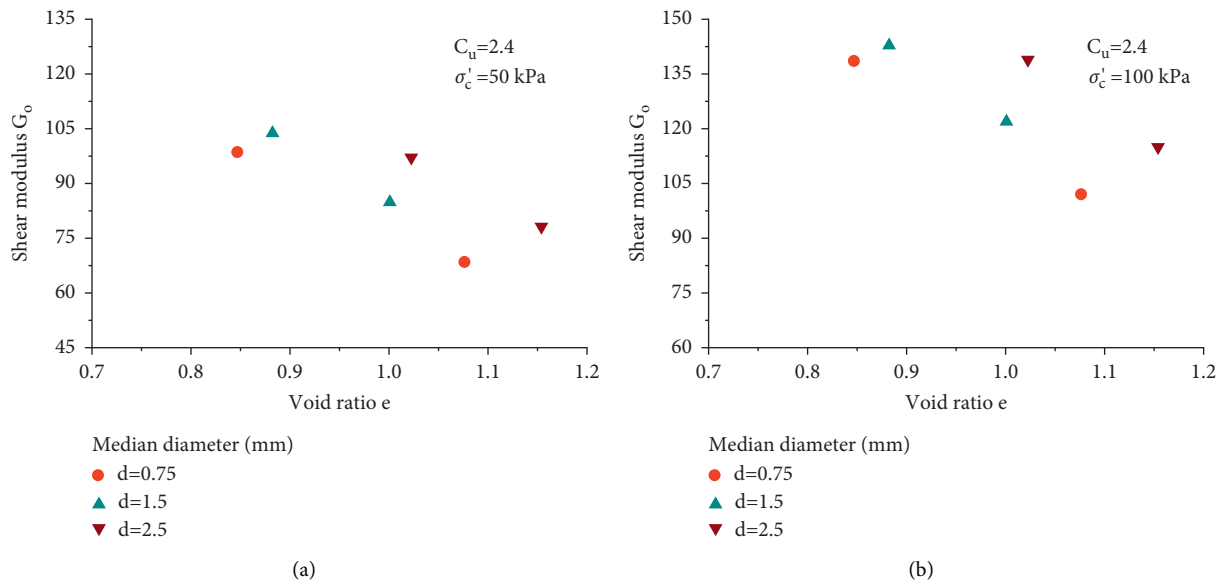

Figure 11: Continued.

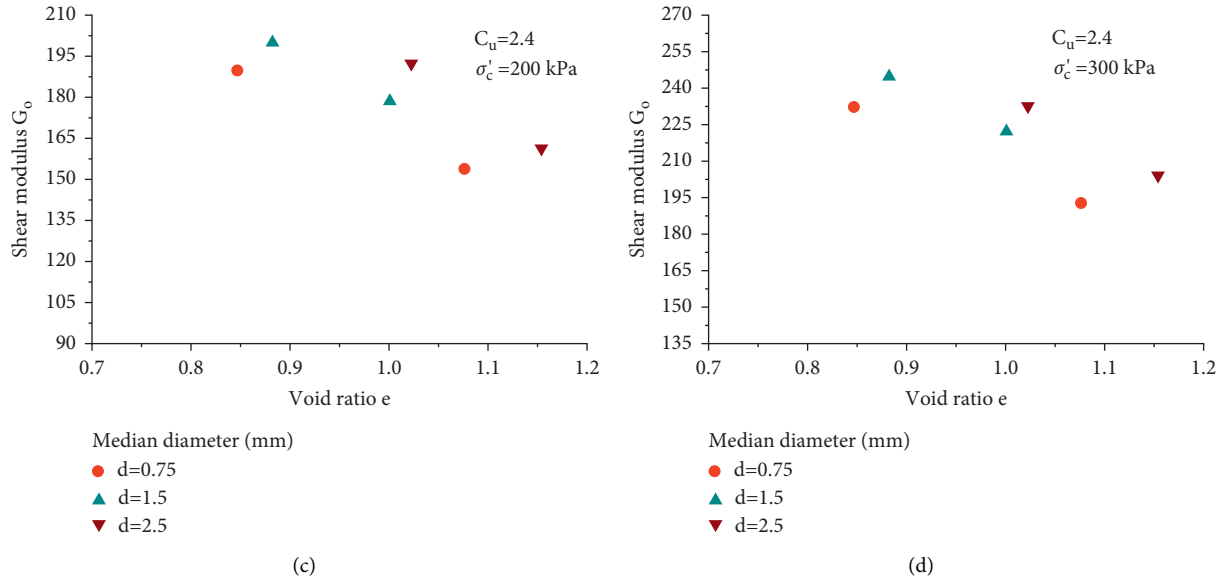

Figure 11: The maximum shear modulus and void ratio for calcareous sand with Cu = 2.4. (a) 50 kPa, (b) 100 kPa, (c) 200 kPa, and (d) 300 kPa.

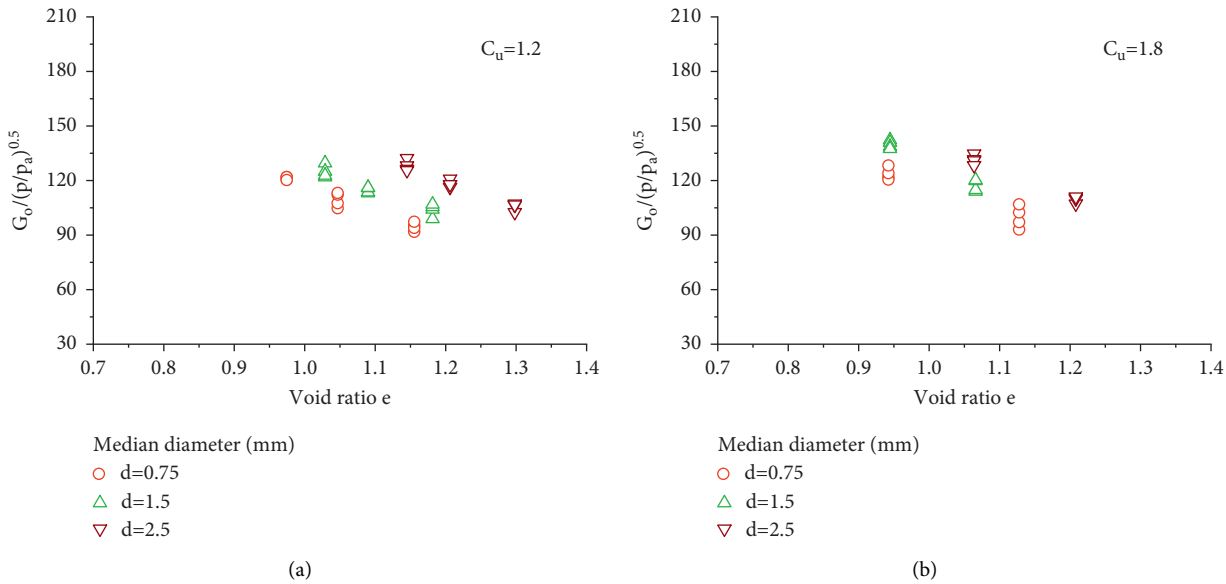

Figure 12: Continued.

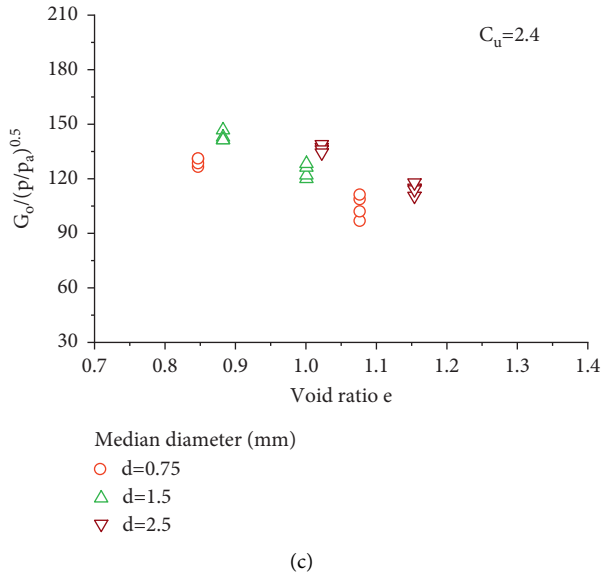

(c)

Figure 12: $G_o/(p/p_a)^n$ and void ratio for calcareous sand at different confining pressure. (a) Cu = 1.2, (b) Cu = 1.8, and (c) Cu = 2.4.

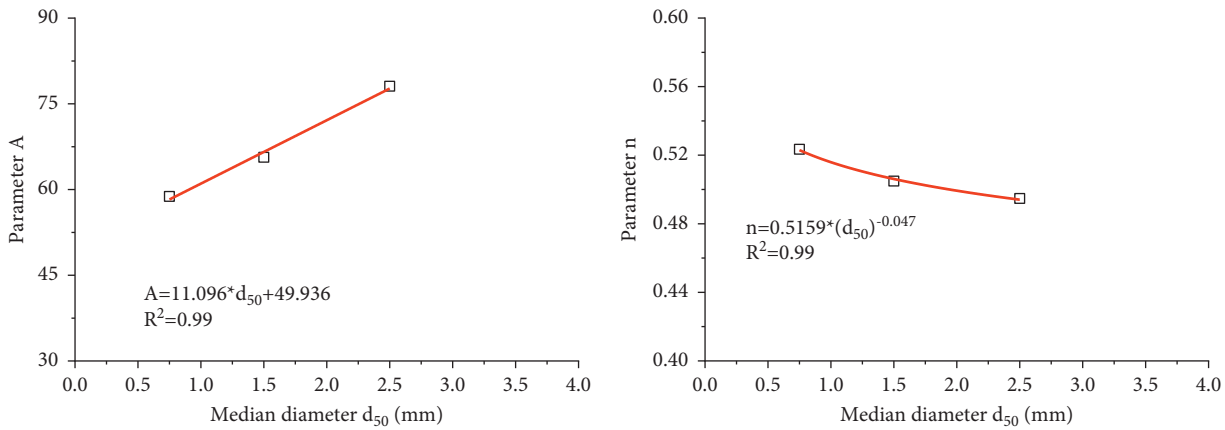

(a) (b)

Figure 13: The median diameter and parameters associated with experienced equations. (a) Parameter A and (b) parameter n.

The test results could be simulated using the Hardin model. However, the model parameters are greatly dependent on the median diameter d_{50}. Therefore, it is necessary to consider the effect of median diameter when the maximum shear modulus is estimated. For calcareous sands with a given median diameter d_{50}, a set of physical parameters including A and n could be obtained.

Figure 13 shows that model parameter A linearly increases with a median diameter of d_{50}. Besides, parameter n has an exponent power relationship with median diameter d_{50}. The goodness of fitting curves in Figure 13 is 0.99. These two parameters can be closely related and expressed using the median diameter d_{50}. Previous studies indicated that parameter c was insensitive to particle characteristics. Thus, parameter c is regarded to be a constant in the prediction.

Figure 14 represents all the test results for calcareous with three grain diameters at different confining pressures and densities. The varying tendency of normalization value of G_o with void ratio e could be described using the unique trend line. The trend line is determined using the revised Hardin model. The physical parameter d_{50} is directly introduced in the Hardin model to quantitatively describe the parameters A and n. Parameters A and n are determined using the best-fitting method to the measured results. The revised Hardin model considering the effect of grain diameter is capable of predicting the maximum shear modulus of calcareous with different gradation conditions at different densities and stresses.

Figures 15 and 16 show the predicted and measured maximum shear modulus of the calcareous sand with varying grading curves under different test conditions. The shear modulus estimated using the original Hardin model is displayed in Figure 15. It is noted that the points representing samples with a median diameter of 0.75 are above

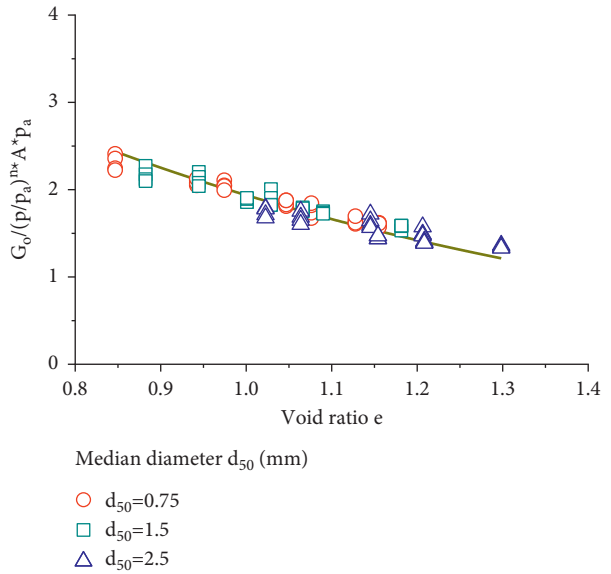

Figure 14: $G_o/(p/p_a)^n A p_a$ and void ratio for calcareous sands with three values of Cu.

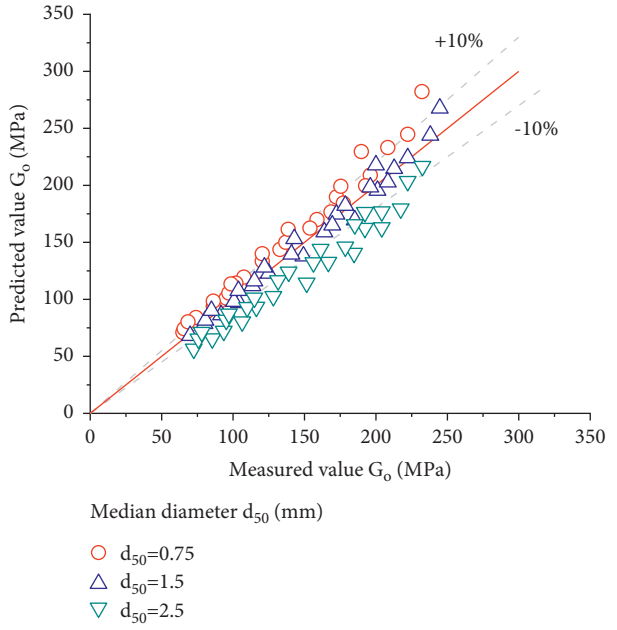

Figure 15: Measured and predicted maximum shear modulus G_o of the calcareous sand with different values of d_{50}.

the test results. It is also seen that the points are out of the zone indicating the relative error value within 10%.

Figure 16 shows that the predicted values match well with measured results with a relative error value of less than 10%. The maximum shear modulus is predicted using the revised Hardin model. The estimation capacity is largely enhanced by considering the influence of the grain size. The calcareous sand ground owns a wide range of grain size distribution curves. The revised Hardin model is expected to provide the predicted maximum shear modulus to accurately reflect the influence of gradation characteristics of calcareous sand ground in engineering practice.

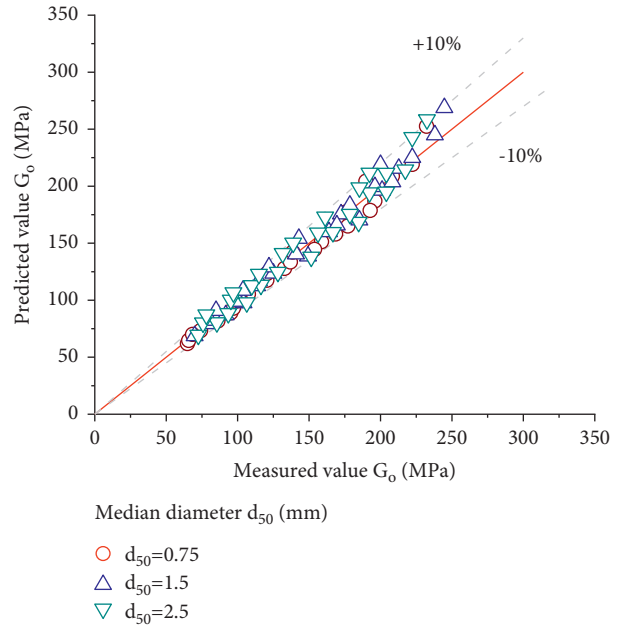

Figure 16: Measured and predicted maximum shear modulus G_o of the calcareous sand using the proposed estimated equation.

5. Conclusions

The grain median diameter is noticed to be an important parameter governing the monotonic and dynamic properties of the calcareous sand. A series of resonant column tests had been conducted to investigate the effect of gradation condition (median diameter and uniform coefficient) on the small-level dynamic property of the calcareous sand under different test conditions. The well-known Hardin model had been revised to include the influence of grain size on the small-level dynamic properties. The new findings of this work can be summarized as follows:

(1) The shear modulus of the calcareous sand tends to decrease with a rise in the shear strain at a given confining pressure and density. The confining stress-dependence and density-dependence of the shear modulus and damping ratio for calcareous sand had been confirmed in this investigation. The maximum shear modulus G_o linearly increases with the level of confining pressure at each relative density. On the maximum shear modulus and void ratio plane, the influence of uniform coefficient Cu on the measured maximum shear modulus is minimal.

(2) On the shear modulus and void ratio plane, at the same confining pressure and uniform coefficient, a rise in the median diameter enhances the maximum shear modulus. The maximum shear modulus displays a decreasing tendency with increasing void ratio. The looser the calcareous sand sample is, the smaller the capacity of the resisting torsion loading becomes.

(3) The physical parameter A in the Hardin model increases with median diameter, while parameter n in

the Hardin model exponentially decreases with the median diameter. The well-proved Hardin equation had been revised to consider the influence of median diameter. The proposed equation is capable of characterizing the small-level dynamic property of the calcareous sand with varying gradation conditions.

Data Availability

The data used to support the findings of this study are available from the corresponding author upon request.

Conflicts of Interest

The author declares no conflicts of interest regarding the publication of this paper.

Acknowledgments

A part of the work was funded by the Scientific Research Fund of Institute of Engineering Mechanics, China Earthquake Administration (Grant no. 2020D01), Guangdong Basic and Applied Basic Research Foundation (2021A1515012096 and 2021A1515110201), and Guangzhou City Technology and Science Program (202102010380 and 202201020204).

References

[1] M. R. Coop and J. H. Atkinson, "The mechanics of cemented carbonate sands," *Geotechnique*, vol. 43, pp. 53–67, 1993.

[2] S. Donohue, C. O' Sullivan, and M. Long, "Particle breakage during cyclic triaxial loading of a carbonate sand," *Geotechnique*, vol. 59, pp. 477–482, 2009.

[3] H. Shahnazari, Y. Jafarian, M. A. Tutunchian, and R. Rezvani, "Undrained cyclic and monotonic behavior of hormuz calcareous sand using hollow cylinder simple shear tests," *International Journal of Civil Engineering*, vol. 14, no. 4, pp. 209–219, 2016.

[4] G. Miao and D. Airey, "Breakage and ultimate states for a carbonate sand," *Géotechnique*, vol. 63, no. 14, pp. 1221–1229, 2013.

[5] Y. Wu, N. Li, X. Wang et al., "Experimental investigation on mechanical behavior and particle crushing of calcareous sand retrieved from South China Sea," *Engineering Geology*, vol. 280, Article ID 105932, 2021.

[6] T. Hyodo, Y. Wu, and M. Hyodo, "Influence of fines on the monotonic and cyclic shear behaviour of volcanic soil "Shirasu," *Engineering Geology*, vol. 301, 2022 https://doi.org/10.1016/j.enggeo.2022.106591, Article ID 106591.

[7] X.-Z. Wang, Y.-Y. Jiao, R. Wang, M.-J. Hu, Q.-S. Meng, and F.-Y. Tan, "Engineering characteristics of the calcareous sand in Nansha islands, South China Sea," *Engineering Geology*, vol. 120, no. 1-4, pp. 40–47, 2011.

[8] X. Wang, H. Shan, Y. Wu, Q. Meng, and C. Zhu, "Factors affecting particle breakage of calcareous soil retrieved from South China Sea," *Geomech. Eng.*vol. 22, pp. 173–185, 2020.

[9] T. Iwasaki and F. Tatsuoka, "Effects of grain size and grading on dynamic shear moduli of sands," *Soils and Foundations*, vol. 17, no. 3, pp. 19–35, 1977.

[10] E. Selig, R. Chung, F. Yokel, and V. Drnevich, "Evaluation of dynamic properties of sands by resonant column testing," *Geotechnical Testing Journal*, vol. 7, no. 2, p. 60, 1984.

[11] D. C. F. Lo Presti, M. Jamiolkowski, O. Pallara, A. Cavallaro, and S. Pedroni, "Shear modulus and damping of soils," *Géotechnique*, vol. 47, no. 3, pp. 603–617, 1997.

[12] K. Senetakis, A. Anastasiadis, and K. Pitilakis, "Normalized shear modulus reduction and damping ratio curves of quartz sand and rhyolitic crushed rock," *Soils and Foundations*, vol. 53, no. 6, pp. 879–893, 2013.

[13] H. H. G. Pham, V. I. Peter, V. I. William, M. Patrick, C. Veerle, and W. Haegeman, "3D particle shape of calcareous sand conducted by X-Ray computed tomography," in *Proceedings of the the 2nd World Congress on Civil, Structural, and Environmental Engineering*, CSEE'17, Barcelona, Spain, April 2017.

[14] M. Goudarzy, M. M. Rahman, D. König, and T. Schanz, "Influence of non-plastic fines content on maximum shear modulus of granular materials," *Soils and Foundations*, vol. 56, no. 6, pp. 973–983, 2016.

[15] M. M. Rahman, M. Cubrinovski, and S. R. Lo, "Initial shear modulus of sandy soils and equivalent granular void ratio," *Geomechanics and Geoengineering*, vol. 7, no. 3, pp. 219–226, 2012.

[16] B. O. Hardin and W. L. Black, "Sand stiffness under various triaxial stresses," *Journal of the Soil Mechanics and Foundations Division*, vol. 92, no. 2, pp. 27–42, 1966.

[17] Y. Jafarian and H. Javdanian, "Small-strain dynamic properties of siliceous-carbonate sand under stress anisotropy," *Soil Dynamics and Earthquake Engineering*, vol. 131, Article ID 106045, 2020.

[18] A. Anastasiadis, K. Pitilakis, K. Senetakis, and A. Souli, "Dynamic response of sandy and gravelly soils: effect of grain size characteristics on G-γ-D curves," in *Proceedings of the the 5th International Conference on Earthquake Geotechnical Engineering*, Santiago, Chile, January 2011.

[19] T. Wichtmann and T. Triantafyllidis, "Effect of uniformity coefficient on G/gmax and damping ratio of uniform to well-graded quartz sands," *Journal of Geotechnical and Geoenvironmental Engineering*, vol. 139, no. 1, pp. 59–72, 2013.

[20] P. H. Ha Giang, P. O. Van Impe, W. F. Van Impe, P. Menge, and W. Haegeman, "Small-strain shear modulus of calcareous sand and its dependence on particle characteristics and gradation," *Soil Dynamics and Earthquake Engineering*, vol. 100, pp. 371–379, 2017.

[21] B. O. Hardin and F. E. Richart, "Elastic wave velocities in granular soils," *Journal of the Soil Mechanics and Foundations Division*, vol. 89, no. 1, pp. 33–65, 1963.

[22] M. Hyodo, Y. Wu, S. Kajiyama, Y. Nakata, and N. Yoshimoto, "Effect of fines on the compression behaviour of poorly graded silica sand," *Geomech. Eng.*vol. 12, no. 1, pp. 127–138, 2017.

[23] N. Yoshimoto, Y. Wu, M. Hyodo, and Y. Nakata, "Effect of relative density on the shear behaviour of granulated coal ash," *Geomech. Eng.*vol. 10, no. 2, pp. 207–224, 2016.

[24] Y. Wu, N. Yoshimoto, M. Hyodo, and Y. Nakata, "Evaluation of crushing stress at critical state of granulated coal ash in triaxial test," *Géotechnique Letters*, vol. 4, no. 4, pp. 337–342, 2014.

[25] Y. Wu, J. Cui, J. Huang, W. Zhang, N. Yoshimoto, and L. Wen, "Correlation of critical state strength properties with particle shape and surface fractal dimension of clinker ash," *International Journal of Geomechanics*, vol. 21, no. 6, Article ID 4021071, 2021.

[26] Y. Wu, H. Yamamoto, and Y. Yao, "Numerical study on bearing behavior of pile considering sand particle crushing," *Geomech. Eng.*vol. 5, no. 3, pp. 241–261, 2013.
[27] M. Hyodo, Y. Wu, N. Aramaki, and Y. Nakata, "Undrained monotonic and cyclic shear response and particle crushing of silica sand at low and high pressures," *Canadian Geotechnical Journal*, vol. 54, no. 2, pp. 207–218, 2017.
[28] M. J. Winter, M. Hyodo, Y. Wu, N. Yoshimoto, M. B. Hasan, and K. Matsui, "Influences of particle characteristic and compaction degree on the shear response of clinker ash," *Engineering Geology*, vol. 230, pp. 32–45, 2017.
[29] Y. Wu, H. Yamamoto, J. Cui, and H. Cheng, "Influence of load mode on particle crushing characteristics of silica sand at high stresses," *International Journal of Geomechanics*, vol. 20, no. 3, Article ID 4019194, 2020.
[30] Y. Wu, M. Hyodo, and N. Aramaki, "Undrained cyclic shear characteristics and crushing behaviour of silica sand," *Geomech. Eng.*vol. 14, pp. 1–8, 2018.
[31] W. Zhang, J. Q. Zou, K. Bian, and Y. Wu, "Thermodynamic-based cross-scale model for structural soil with emphasis on bond dissolution," *Canadian Geotechnical Journal*, vol. 59, no. 1, pp. 1–11, 2022.
[32] Y. Jafarian, H. Javdanian, and A. Haddad, "Dynamic properties of calcareous and siliceous sands under isotropic and anisotropic stress conditions," *Soils and Foundations*, vol. 58, no. 1, pp. 172–184, 2018.
[33] S. Oztoprak and M. D. Bolton, "Stiffness of sands through a laboratory test database," *Géotechnique*, vol. 63, no. 1, pp. 54–70, 2013.
[34] C. Zou, J. A. Moore, M. Sanayei, Z. Tao, and Y. Wang, "Impedance model of train-induced vibration transmission across a transfer structure into an over track building in a metro depot," *Journal of Structural Engineering*, vol. 172, pp. 739–750, 2022.
[35] H. Jin, Q. Tian, and Z. Li, "Crack development of rebar rust in rubberized concrete using mesoscale model," *Construction and Building Materials*, vol. 321, Article ID 126409, 2022.
[36] L. H. Xu and M. Ma, "Dynamic response of the multilayered half-space medium due to the spatially periodic harmonic moving load," *Soil Dynamics and Earthquake Engineering*, vol. 157, Article ID 107246, 2022.
[37] H. Jin, J. Su, and C. Zhao, "Relationship between invert-filling disengaging and deformation of shield tunnel using staggered assembled segment," *KSCE Journal of Civil Engineering*, vol. 26, no. 4, pp. 1966–1977, 2022.
[38] M. Ma, M. H. Li, X. Y. Qu, and H. Zhang, "Effect of passing metro trains on uncertainty of vibration source intensity: monitoring tests," *Measurement*, vol. 193, Article ID 110992, 2022.
[39] B. Yuan, Z. Li, Y. Chen et al., "Mechanical and microstructural properties of recycling granite residual soil reinforced with glass fiber and liquid-modified polyvinyl alcohol polymer," *Chemosphere*, vol. 286, Article ID 131652, 2022.
[40] B. Yuan, Z. Li, W. Chen et al., "Influence of groundwater depth on pile–soil mechanical properties and fractal characteristics under cyclic loading," *Fractal and Fractional*, vol. 6, no. 4, p. 198, 2022.
[41] B. Yuan, M. Chen, W. Chen, Q. Luo, and H. Li, "Effect of pile-soil relative stiffness on deformation characteristics of the laterally loaded pile," *Advances in Materials Science and Engineering*, vol. 2022, p. 13, Article ID 4913887, 2022.
[42] B. Yuan, W. Chen, J. Zhao, F. Yang, Q. Luo, and T. Chen, "The effect of organic and inorganic modifiers on the physical properties of granite residual soil," *Advances in Materials Science and Engineering*, vol. 2022, Article ID 9542258, 13 pages, 2022.
[43] B. Yuan, Z. Li, Z. Zhao, H. Ni, Z. Su, and Z. Li, "Experimental study of displacement field of layered soils surrounding laterally loaded pile based on Transparent Soil," *Journal of Soils and Sediments*, vol. 21, no. 9, pp. 3072–3083, 2021.